3D modeling to evaluate the thermal interferences between borehole heat exchangers in a Mediterranean area

Vitriu, E.,[1], Arnó, G.,[2], Herms, I.,[2], De Felipe, J.J.[3]

[1] Master's Degree in Energy Engineering, Universitat Politècnica de Catalunya, Av/ Diagonal 647, Barcelona, Spain

[2] Àrea de Recursos Geològics, Institut Cartogràfic i Geològic de Catalunya (ICGC), Parc de Montjuïc s/n, 08038, Barcelona, Spain

[3] Departament of Mining, Industrial and ICT Engineering. Universitat Politècnica de Catalunya, Av/ Bases de Manresa 61-73, Manresa, Barcelona (Spain)

ignasi.herms@icgc.cat

Keywords: Modeling, borehole heat exchanger, thermal interference, Feflow.

ABSTRACT

Thermal interference between Borehole Heat Exchangers (BHEs) results in a loss of performance of a geothermal installation. An analysis of this phenomenon can provide key information for enhance and optimize the design of a closed-loop geothermal system. To study this thermal effect in the subsoil, a simulation tool is needed to solve numerically the equations of flow and heat transport in a porous medium.

The main objective of this research is to analyze and compare the influence of the distance between different BHE in three types of geometrical arrays using a 3D finite element modelling software. By fixing the heating and cooling demand of a group of single-family houses, different numbers of vertical BHEs in a closed-loop system with simple parallel U-tubes were simulated.

The 3D finite elements model was performed including the geological and hydrogeological settings of the northern part of Valencia city (SE, Spain) situated in the Mediterranean area. The applied geological, hydrogeological and thermal conceptual model is based on previously available information.

The thermal model was calibrated in transient state with two different datasets: a set of operating data of a monitored shallow geothermal installation located in the ETSII-UPV (*Escuela Técnica Superior de Ingenieros Industriales - Universidad Politécnica de Valencia - UPV*), and data of a Thermal Response Test (TRT) did at the same area. The resulting model set the initial conditions to model the thermal interference between the different BHEs arrays. The studied configurations were matrices of 2, 4 and 9 BHEs, with variable distances between 3 and 20 m.

The radius of thermal perturbation on the subsoil for each array of BHEs simulated was determined and the variation of the performance was characterized.

The simulation results showed that there was a slight increase in temperature in the subsoil between the BHEs and its surroundings. Thermal interference was usually not visible in the first year, but in a long-term analysis, for a certain range of distances between BHEs, it was observed that a hot area appeared. The temperature increase calculated in one layer at an average depth was reproduced for different types of arrays.

Even though the experimental data and the simulated scenarios corresponds to a specific place in Valencia City, the methodology scheme applied could be used in other cases, helping to understand the subsoil and BHEs behavior from a long-term point of view.

1. INTRODUCTION

The building sector is the largest energy consumer sector, accounting for over one-third of the final energy consumption in the world. In the EU, it is responsible for 40% of the total energy consumption (European Parliament, directive 2012/27/EU) of which heating, cooling and hot water represent approximately 70% (IEA, 2013). Currently, around 75% of the primary energy supply for heating and cooling is based on fossil fuels (Council European Parliament, 2016). Furthermore, buildings are responsible of 30% of annual greenhouse gas emissions. The United Nations Environmental Program states that carbon dioxide emissions from residential buildings are rising at a rate of 1.7% each year (Houvila et al, 2013).

In this context, shallow geothermal energy represents a renewable energy source with a vast potential of energy savings for heating and cooling of buildings, which could achieve up to 70% energy savings compared to traditional systems (EGEC, 2015).

In the absence of any official inventory in the autonomous community of Valencia, the IDAE (2011) estimated that at least 1.4 MWt of shallow geothermal potential has been installed. This is a rather low value compared to other Spanish autonomous communities, Catalonia (with at least 27 MW) or other European countries. Therefore, Valencia is one of the regions with better perspectives in shallow geothermal energy use growth.

The city of Valencia, were this research is focused, is located in the eastern Mediterranean coast of Spain (Fig. 1). The climate is temperate with an average winter temperature ranges between 10 and 13ºC while the average summer temperature ranges between 21 and 25ºC. The total average annual precipitation is about 475 mm.

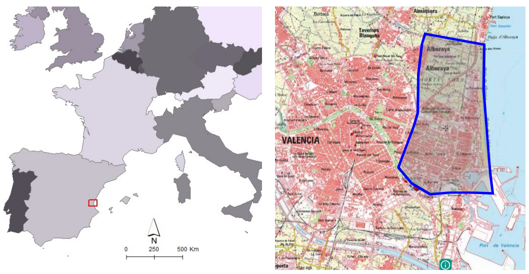

Figure 1: Study area. The city of Valencia and the area were the 3D model was performed.

A PhD program developed in the Polytechnical University of Valencia (Magraner, 2010), aimed to validate the tools for the design of ground coupled heat pump systems using experimental data from a pilot monitored installation located near the UPV campus in Valencia city. In this research Magraner (2010) pointed out that the thermal interference between BHEs is a design parameter that had to be taken into account.

Generally, during the sizing of a vertical geothermal Borehole Heat Exchanger (BHE) for residential buildings, it is assumed that there is no interference between the probes (ACTECYR, 2012). This means that the variations in subsoil temperatures caused by a nearby BHE are not considered.

The interference between the BHEs produces a loss of the performance of the installation, which means that not all the energy expected to feed the building is covered, so an additional cost not expected will be required. One alternative could be separate the BHEs a larger distance, but it would result in an increasing of the pressure and temperature losses in the surface piping, an increasing of the soil area necessary to install the BHEs and thus an increasing of the economic costs of the installation. A previous analyze and description of the interference phenomenon will allow a good sizing and evaluation of a geothermal installation. In that sense, this research presents a methodology scheme that can be useful and applicable to other locations.

A 3D finite elements model had been performed as a tool for long-term shallow geothermal exploitation simulations by combining the experimental data from the UPV and the geological and hydrogeological knowledge of Valencia City. This allowed evaluating and characterizing thermal interferences and quantifying the loss in performance depending on the number and distance between BHEs for a simulated group of single-family houses in Valencia City

2. LITERATURE REVIEW

It is possible to find numerous articles that describe the modeling of a vertical BHE, for example in the reference (Koohi-Fayegh Rosen, 2013) in which the authors pose the importance of modeling GSHP systems from a variety of aspects, such as sustainability of geothermal systems or their potential impacts on the ecosystems nearby. In heating or cooling dominated climates, an annual energy imbalance is placed on the ground loop and thermal imbalances could cause significant issues with a heat pump's long-term sustainable performance if not properly considered at the design phase.

Hein et al. (2016) study the long-term evolution of the subsurface temperature field varying parameters like subsurface thermal conductivity and groundwater flow velocity. Additionally, two configurations with multiple GSHP systems are analyzed. Although an estimate of the disturbance of the terrain is proposed, the simulations are not carried out, varying the distance between the BHEs. Something similar (distance between BHEs fixed) happens with the article of reference (Miglani et al, 2018) in which a methodology is developed to calculate the long-term geothermal energy potential for an urban neighborhood. A model that accounts the thermal interference between neighboring BHEs is developed in order to simulate their operation and calculate their long-term geothermal energy potential; the method is applied to an urban neighborhood in Zurich, Switzerland with 170 buildings; and results show that the geothermal energy potential is overestimated if thermal interference between BHEs are not accounted for Miglani et al (2018).

Koohi-Fayegh and Rosen (2014) conclude that the possibility of thermal interaction between two neighboring systems exists when systems are installed relatively close to each other. It is estimated however that the thermal interaction between the systems that are installed closely will not be large enough to cause Coefficient of Performance (COP) drops of more than 10%. Although in this case a variation of the distance between two BHEs is made, the modeled geothermal demand is balanced (equality of annual energy injected and extracted) and the installation is located in a cold climate zone of Canada.

Law and Dworking (2016) prove that the distance recommended by ASHRAE (6 m), is not always sufficient to prevent borehole thermal interactions. In the reference (Law and Dworking, 2016) it is well studied the long-term ground temperature response using finite-element methods for four kinds of buildings with different energy balances varying borehole configurations. In this study, the distance between the BHEs is fixed, groundwater movement was assumed negligible and COP was set constant.

Gultekin et al. (2016) propose to determine the optimal distance between BHEs calculating the performance loss due to mutual thermal interactions of BHEs, the averaged Heat Transfer Rate value of the most critical BHE in each configuration is compared with that of a single borehole alone for various borehole spacing and operation durations of 1800 and 2400h (only heating mode).

3. THE 3D MODEL

3.1 Model construction

The 3D finite element model used in this research was developed using the software Feflow (DHI) v.7.1.

The domain and flow boundary conditions of the model were determined from IGME (2015) (Figure 2). The northern and southern limits are considered as no-flow boundaries. In the W and E limits of the model, fixed hydraulic head (1st kind/Dirichlet boundary condition) are considered respectively: 1 m.a.s.l. and 0 m.a.s.l. at the coastal line.

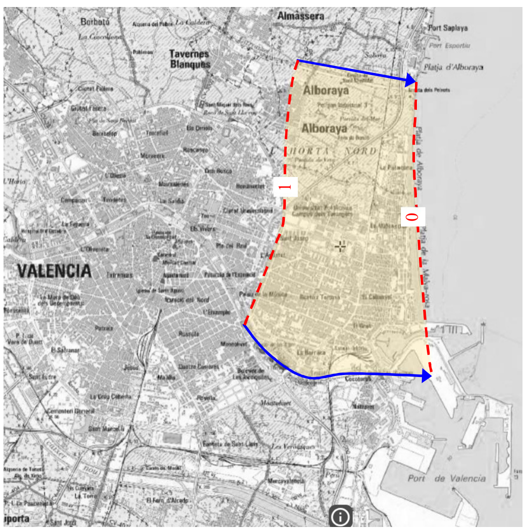

Figure 2: Maps composition: City of Valencia, blue lines are the northern and southern limits of the model, and red dashed lines the piezometric western and eastern limits. The study area is pointed out in yellow shadow.

For spatial discretization of the model domain, 4000 finite elements (triangular shapes) were used. In the area where the BHEs had to be inserted the mesh was refined with higher discretization in order to enhance the computation. The resulting 2D mesh can be observed in Figure 3.

The conceptual geological model was established considering Magraner (2010), Ballesteros et al (2007), and DGA (2015). The implemented geological model considers 3 layers:

1. A surficial layer with a thickness of 50 m composed of a mixture of gravel and saturated clays. It corresponds to the depth at which the UPV's geothermal BHEs are located.

2. The bottom of the second layer was set at 100 m.b.s.l., and represents a BHE of 109 m deep. This corresponds to the depth of the TRT performed in the area.

3. A third layer was proposed as a backstay with a thickness of 100 m with the same characteristics to the previous one.

The model domain is enough to avoid interference problems with the boundaries. That means the boundaries are far away enough to not interact with the thermal perturbation generated around the BHEs location.

For the resolution of heat transport process, it was established an initial average temperature of 20.2ºC (Magraner, 2010) to the control volume. Table 1 shows the flow and heat parameters of the subsoil (porous media) assigned to each layer.

Table 1: Material properties for flow and heat transport for each layer.

		Layer Nº	1	2	3
		Thickness [m]	50	59	100
Matrix	Hydraulic Properties	Hydraulic conductivity [m/d]	10	4.2	2.5
		Storage Coefficient [%]	7	0.1	0.1
	Thermal Properties	Volumetric Heat Capacity [MJ/m3K]	2.4	2.5	2.5
		Thermal Conductivity [W/mK]	1.4	2.1	2.1
Fluid	Thermal Properties	Volumetric Heat Capacity [MJ/m3K]	4.2	4.2	4.2
		Thermal Conductivity [W/mK]	0.6	0.6	0.6

The first step was to calculate the steady-state flow and thermal conditions (Figure 4).

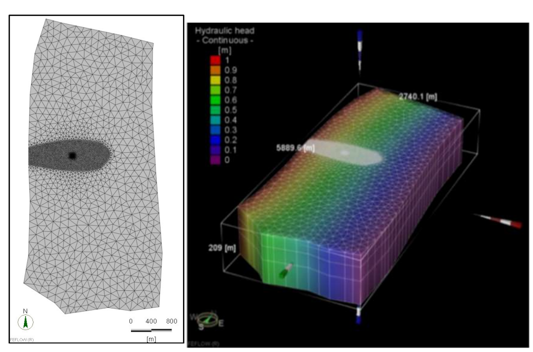

Figures 3 and 4: 2D mesh and steady-state flow conditions

The second step was to calibrate the model in transient state assuming that the initial conditions for the flow simulation reflect the steady-state conditions.

3.2 Model calibration

The transient calibration of heat transport was done using the trial-and-error approach, by introducing a BHE, of which experimental data were available, and comparing with the simulated data. To perform the calibration, it was used two available experimental datasets of the area under study. The main data needed were the inlet temperature to the BHE, the flow rate and the outlet temperature.

- 1rst dataset: Geothermal installation in the ETSII-UPV of 6 BHEs of 50 m deep distributed in a rectangular way (2 x 3). They had two temperature sensors in each BHE (sensors are generally available at the input and output of the array) which were necessary for the validation of the model. The available data were from July 2006 (cooling mode) but only the period between days 20 and 31 was taken for the analysis, since more stable flow and temperature behavior was observed.

- 2n dataset: TRT data performed in the same area in the ETSII-UPV on December 2015. It was performed in a BHE of 109 m deep and consisted of a heat injection to the ground.

In both cases, the same simple U pipe with the following characteristics was used (see Table 2 and Figure 5).

Table 2: Characteristics of the BHEs.

Geometrical Parameters		
BHE Geometry	Single U-shape	
Borehole Diameter (D)	0.12	m
Pipe Distance (w)	0.07	m
Pipe Diameter (d)	0.032	m
Pipe Thickness (b)	0.0029	m
Thermal Properties		
Pipe Thermal Conductivity	0.42	W/mK
Grout Thermal Conductivity	2	W/mK
Grout Heat Capacity	2.2	MJ/m3K
Refrigerant Heat Capacity	4.18	MJ/m3K
Refrigerant Thermal Conductivity	0.597	W/mK
Refrigerant Viscosity	1·10-3	kg/ms
Refrigerant Density	1000	kg/m3

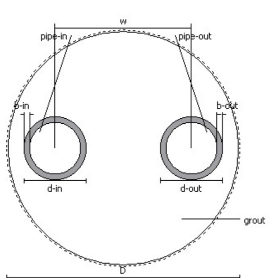

Figure 5: View of the BHE scheme and grout with the single U-pipe.

Figure 6 shows the results obtained during the calibration process using the 1rst dataset (experimental for a period of 11 days). From day number 7 a good adjustment in temperature and power is observed. The installation had been operating for about two years before (not continuously) and therefore the ground around it must have already been disturbed (by the same BHE and the others). In the simulation, at the beginning of the calculations, the subsoil was considered without alterations. That could explain the difference observed during the first days. Finally, taking all these considerations into account, a good overall fit can be assumed with this experimental data.

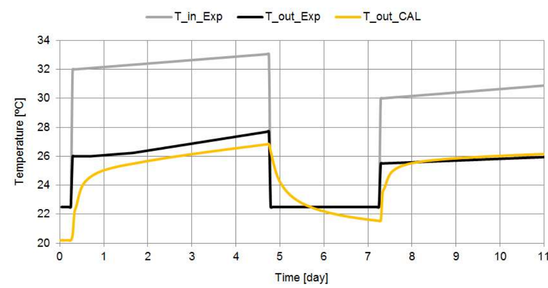

Figure 6: UPV Experimental and simulated temperature (T_in_Exp: inlet temperature – T_out_Exp: outlet temperature – T_out_CAL: simulated outlet temperature).

Figure 7 shows the results obtained during the calibration process using the 2n dataset (TRT data). It is shows a very good fit between observed and simulated data.

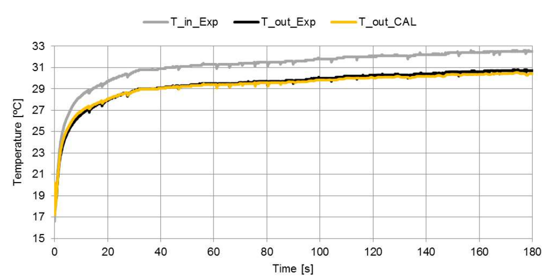

Figure 7: TRT Experimental and simulated temperature (T_in_Exp: inlet temperature – T_out_Exp: outlet temperature – T_out_CAL: simulated outlet temperature).

Table 1 already reflects the final parameter estimations after model calibration.

4. CASE STUDIES

After the calibration process, three scenarios were proposed based on the annual energy demand of a group of houses and the number of BHEs to cover it. In each of these scenarios, the distance between the BHEs was varied in order to evaluate how the interference affects the total amount of energy exchanged between the BHEs and the terrain.

The number of houses is like a multiplying factor of the energy demand and peak power of one single house

(See Table 4). It was assumed that the houses were sufficiently separated so that one does not affect the energy demand of the other.

The following Table 3 summarizes the case studies considered:

Table 3: Case studies.

Name	Nº Houses	Nº BHEs	Array Distribution	Distances between BHEs [m]
Low	2	2	1 x 2	3, 6, 9, 12, 15, 18 and 20.4
Medium	4	4	2 x 2	3, 6, 9, 12, 15, 18 and 21
High	8	9	3 x 3	3, 6, 9, 12, 15, 18 and 21

Table 4: Maximum thermal power and annual energy demand for each scenario.

			Max Power		Annual Energy	
Demand	Array	Dwelling	Heating	Cooling	Heating	Cooling
Name	Nº BHEs	Nº Houses	P_{LH} $[kW]$	P_{LC} $[kW]$	E_{LH} $[MWh]$	E_{LC} $[MWh]$
Low	2	2	-8.1	6.6	-8.1	6.5
Medium	4	4	-16.2	13.3	-16.2	12.9
High	9	9	-32.5	26.6	-32.3	25.9

Special geographical distributions of the BHEs in the land were:

- For the case of medium and high demand (4 and 9 BHEs) it was necessary to use a grid distribution that allowed studying the interference between the BHEs in a more symmetrical way.
- It was considered that a distance of more than 20 m would be enough for the thermal interference between BHE to be negligible.

To cover the building heating and cooling power demand in each scenario, a heat pump was selected. According the Spanish Norm (AENC, 2014) the operational range of the heat pump for residential heating and cooling, corresponds to low power (less than 30kW).

With the data of the heat pump and the energy and power of the energy demand of the buildings, the power and thermal energy injected or extracted from the ground were estimated as a function of the outside temperature for the period of one climatological year of Valencia (RETScreen International, 2005).

This allowed to determine the flowrate of water and the temperature difference of the water injected / extracted from the BHEs, which were the variables introduced in the model to study the thermal interference between them.

Once the annual energy demand curve for each scenario had been obtained, it was extended by the full lifetime of the geothermal installation, which according to consulted sources (Hein et al, 2016) and (García-Gil et al, 2015) can reaches up to 30 years. The model proposed in Feflow was adapted for each scenario by changing the number and distance between the BHEs. For each period (annual) an average flow and inlet temperature values were used (Table 5).

Table 5: Average flow rate and inlet temperature during one year considered during the simulation of the study cases.

	2 BHEs (Low)		4 BHEs (Medium)		9 BHEs (High)	
Time	Rate Ave	T_in Ave	Rate Ave	T_in Ave	Rate Ave	T_in Ave
days	m^3/d	ºC	m^3/d	ºC	m^3/d	ºC
0 - 138	3.8	13	8.8	13	20.0	13.5
138–298	7.9	28	13.9	29	29.0	28.5
298-365	3.9	14	8.9	14	19.2	14.5

5. RESULTS

5.1 Energy interference results

It was considered that 100% of the energy that must be injected (cooling) and extracted (heating) by the BHEs during the 30 years of the installation lifetime corresponds to a distance between boreholes of more than 20 meters (negligible or no interference scenario). In the graphs of Figure 8 and Figure 9, it is possible to see how much of this value is covered by decreasing the distance between the BHEs for the three types of array studied: 2, 4 (2 x 2) and 9 (3 x 3) BHEs. While the covered cooling energy increases with the distance between BHEs, the heating energy presents a maximum increase between 6 and 9 m due to a higher temperature zone that is not dissipated from the previous cooling period (Fig.9).

It is possible to see that the worst scenario for all configurations is when the distance between BHEs is 3m. The array of 9 BHEs is the most affected, presenting a reduction of almost 10% for cooling and 4% for heating, compared to the case of non-interference. For distances equal and greater than 6 m, the percentage covered by cooling is above 98%.

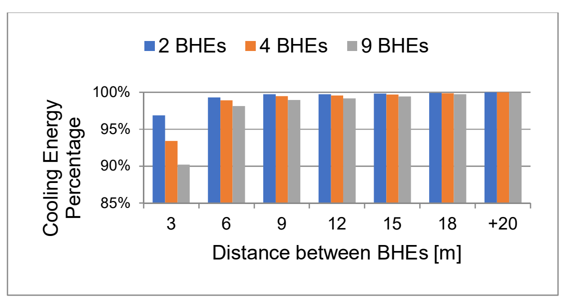

Figure 8: Covered cooling energy versus distance between BHEs for the three arrays in 30 years.

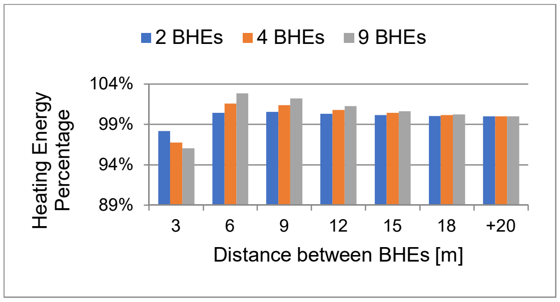

Figure 9: Covered heating energy versus distance between BHEs for the three arrays in 30 years.

Although in the three types of array the power per BHE or per linear meter of depth is similar, it is distinguished that the distribution most affected by the interference phenomena is that of 9 BHEs, then that of 4 BHE and finally that of 2 BHE. This means that the parameter to be taken into account is the total power of the group of the probes and not their individual contribution. As a general rule it is observed that an increase in the power of the array (or number of BHEs) means an increase in the interference effect.

There is a decrease in the balance of energy exchanged between the BHEs and the terrain due to the interference that is generated by decreasing the distance between BHEs. The point of energy balance at the end of the useful life of the installation corresponds to the sum of the cooling and heating energy exchanged with the ground during the 30 years of operation.

Therefore, it can be calculated for all the scenarios, taking as reference the case of non-interference, how far the curves are separated at this point; and this ratio can be considered as a type of "interference efficiency" of the geothermal array (See [1]). In the plot of the Figure 10 it could be seen these calculations and how they fit very well to expressions of the logarithmic type (Table 6).

$$\eta_{Interf} = \left.\frac{E_{BCE\_D}}{E_{BCE\_NI}}\right|_{\substack{30\ years \\ N}} = \left.\frac{E_{H\_D} + E_{C\_D}}{E_{H\_NI} + E_{C\_NI}}\right|_{\substack{30\ years \\ N}} \quad [1]$$

Where:

η_Interf: Interference Efficiency

E_(BCE_D): Geothermic energy balance in 30 years with a distance D between the BHEs.

E_(BCE_NI): Geothermic energy balance in 30 years, Non-Interference condition (distance between BHEs more than 20m).

E_(H_D): Total heating energy in 30 years with a distance D between the BHEs

E_(C_D): Total cooling energy in 30 years with a distance D between the BHEs

E_(H_NI): Total heating energy in 30 years with in non-interference condition

E_(C_NI): Total cooling energy in 30 years with in non-interference condition

D: Distance between BHEs [m]

N: Number of BHEs in the array

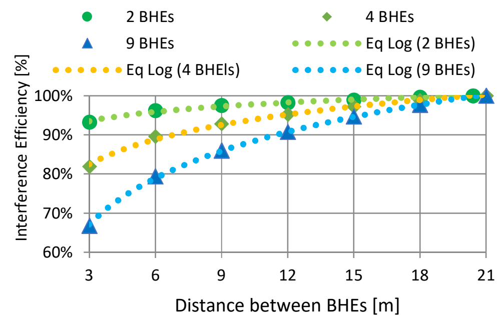

Figure 10: Variation of the energy balance at the end of the useful life of the installation.

Table 6: Logarithmic equations that adjust the interference efficiency for each array.

Array	Equation	Error
2 BHEs	η_{Interf}=0.0344*ln(D)-0.1029	R^2=0.992
4 BHEs	η_{Interf}=0.0916*ln(D)-0.2757	R^2=0.9954
9 BHES	η_{Interf}=0.1706*ln(D)-0.5162	R^2=0.9995

With these equations it will be possible to estimate, for this particular case, how far from the design case is an installation due to interference effects as a function of the distance between BHEs.

5.2 Temperature interference results

The effects on the ground temperature were studied in the layer at middle depth of 50 m.

The thermal disturbance radius for 9 BHEs (3x3) was calculated and mapped for different distances (Fig. 11). The geometry of the thermal disturbance is clearly affected by the groundwater flow existing in the area from west to east. It also can be clearly seen that when the distance between BHEs is greater or equal to 9 m, the disturbance radius is slightly affected with an increase in the distance between boreholes. This could explain how it was seen above, that from 9 m the interference phenomenon can be considered almost negligible, since the maximum area of energy exchange with the subsoil has been reached.

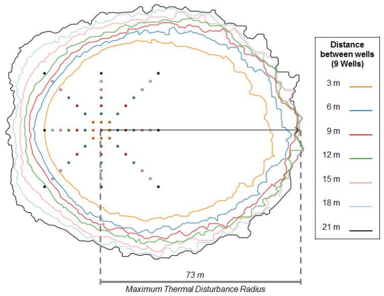

Figure 11: Thermal Disturbance radius for 0.1ºC on the last day of the 30th year for array of 9 BHEs in the layer at 50m of depth

Subsoil temperature maps for each scenario were generated for the last day of the 30[th] year of the installation lifetime (Fig. 12). An increase of the subsoil temperature can be observed as the total amount of heat injected to the ground during the cooling seasons is higher than the total heat extracted from the ground during the heating seasons.

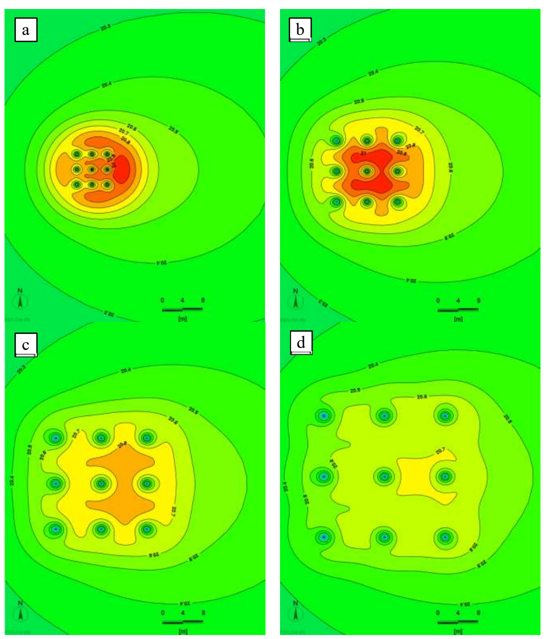

Figure 12: Subsoil temperature maps on the last day of the 30th year at 50 m depth for the array of 9 BHEs. a) at 3 m distance, b) at 6 m distance, c) at 9 m distance, d) at 12 m distance.

As expected, the maximum temperature difference that is generated in the terrain after 30 years occurs in the case of 9 BHEs at 3 m distance (Fig 13).

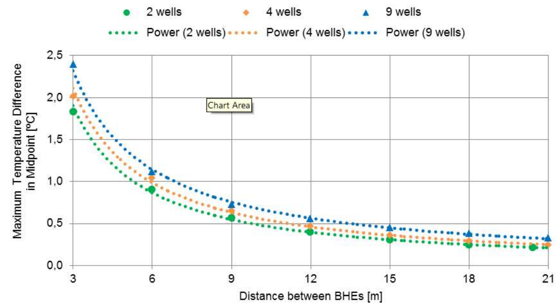

Figure 13: Temperature increase according to the distance between the BHEs for each array.

These results can be used to determine the optimal distance between the BHEs, minimizing the temperature increase in the subsoil, the land surface necessary, and the economic costs.

6. CONCLUSIONS

This work has the novel contribution of studying in the long-term (30 years) the phenomenon of thermal interference between buried geothermal heat exchangers, varying the distance between them, under the premises of Mediterranean warm climate and unbalanced energy demand; and taking into account operating parameters of the heat pump (COP variable with temperature and variable circulation flow in control algorithm) and the thermal and flow hydrogeological parameters of the subsoil. This combination of conditions has not been found in the literature and has the great advantage that it closely approximates the particularities of real geothermal installations in the region.

The main objective of the work was achieved; it was possible to develop an accurate model of the behavior of different BHEs arrays and to deeply study the thermal interference between them. The data used correspond to a specific zone in Valencia City, consequently the numerical results and conclusions can only be understood within this geographical context, but it is important to highlight that this methodology can be applied in a general way.

A valid model of the subsoil was successfully built to solve the transport equations in a meshed control volume applying finite elements methodology.

The behavior of 2, 4 (2 x 2) and 9 (3 x 3) BHEs arrays were studied with the aim of cover the thermal energy demand (heating and cooling) of sets of simple, functional and economic single-family houses. It was evaluated how much of the calculated demand can effectively satisfy the subsoil under conditions of non-interference (distance between BHEs of 20m); for 2-BHEs array, 92% of the cooling and 95% of the heating; for a 4-BHEs array, 94% of the cooling and 99% of the heating; for 9-BHEs array, 97% of the cooling and 100% of the heating.

The worst scenario for all configurations is when the distance between BHEs is 3m. The array of 9 BHEs is the most affected, presenting a reduction of almost 10% for cooling and 4% for heating, compared to the case of non-interference. There is an increase in the interference effect with an increase in array size, although in all scenarios the power per BHE is similar.

The interference efficiency parameter is defined. It should be understood as a factor that indicates how far from the ideal design case is the geothermal installation. The calculations performed show a good logarithmic correlation between this variable and the distance between the BHEs for each type of array. It is also roughly observed that the parameters of the equations found could have a certain mathematical relationship with the number of BHEs of each array. Thereby, it is possible to estimate the interference efficiency for any distance and number of BHEs within the range of study and under the pre-established conditions.

REFERENCES

Asociación Española de Normalización y Certificación. UNE 100715-1 Diseño, ejecución y seguimiento de una instalación geotérmica somera [Internet]. (2014) Available from: http://www.aenor.es/aenor/normas/normas/fichanorma.asp?tipo=N&codigo=N0052899#.WyD-AFUzZpg

Asociación Técnica Española de Climatización y Refrigeración (ATECYR). Guía técnica de diseño de sistemas de intercambio geotérmico de circuito cerrado. Instituto para la Diversificación y Ahorro de la Energía (IDAE); 2012.

Ballesteros, B., Pernía, J.M., Domínguez, J.A., Diaz, E., Espinós, T., Blázquez, E., 'Comportamiento de los acuíferos ante las actuaciones de sequía en los sistemas de explotación Júncar y Turia' (2007). Available from: http://info.igme.es/SidPDF/133000/433/133433_0000001.pdf

Dirección General del Agua. Demarcación hidrográfica del Júcar, Masa de agua subterránea, Plana de Valencia Norte. (2015).

European Geothermal Energy Council (EGEC) B, Universidad Politécnica de Valencia (UPVLC) S, Romanian Geoexchange Society (RGS) R, et al. Developing Geothermal Heat Pumps in Smart Cities and Communities (REGEOCITIES) (2015) Available from: http://regeocities.eu/es/proyect-concept/

European Parliament. Directive 2012/27/EU on Energy Efficiency. Official Journal of the European Union Available from: https://eur-lex.europa.eu/legal-content/EN/TXT/?uri=celex%3A32012L0027

García-Gil A, Vázquez-Suñé E, Schneider EG, Sánchez-Navarro JÁ, Mateo-Lázaro J. Relaxation factor for geothermal use development - Criteria for a more fair and sustainable geothermal use of shallow energy resources. Geothermics, (2015)

Gultekin A, Aydin M, Sisman A. Thermal performance analysis of multiple borehole heat exchangers. Energy Conversion and Management, (2016)

Hein P, Zhu K, Bucher A, Kolditz O, Pang Z, Shao H. Quantification of exploitable shallow geothermal energy by using Borehole Heat Exchanger coupled Ground Source Heat Pump systems. Energy Conversion and Management, (2016)

Hein P, Zhu K, Bucher A, Kolditz O, Pang Z, Shao H. Quantification of exploitable shallow geothermal energy by using Borehole Heat Exchanger coupled Ground Source Heat Pump systems. Energy Conversion and Management, (2016)

Houvila Pekka, Ala-Juusela M, Melchert L, Pouffary S, Cheng C-C, Urge-Vorsatz D, Koeppel S, Svenningsen N, Graham P. Buildings and climate change [Internet]. United Nations Environment Programme; (2013), Available from: http://www.greeningtheblue.org/sites/default/files/Buildings and climate change_0.pdf

IDAE. Evaluación del potencial de energía geotérmica. Estudio Técnico PER 2011-2020, Madrid, (2011), 236 pp.

IGME. Apoyo a la caracterización adicional de las masas de agua subterránea en riesgo de no cumplir los objetivos medioambientales en 2015. Demarcación Hidrográfica del Júcar. Plana de Valencia Norte. *Ministerio de Medio Ambiente y Medio Rural y Marino, (2015), 87 pp.*

International Energy Agency. Transition to sustainable buildings: Strategies and opportunities to 2050 [Internet]. 2013. Available from: https://www.iea.org/publications/freepublications/publication/Building2013_free.pdf

Koohi-Fayegh S, Rosen MA. A review of the modelling of thermally interacting multiple boreholes. Sustainability (Switzerland), (2013)

Koohi-Fayegh S, Rosen MA. An analytical approach to evaluating the effect of thermal interaction of geothermal heat exchangers on ground heat pump efficiency. Energy Conversion and Management, (2014)

Law YLE, Dworkin SB. Characterization of the effects of borehole configuration and interference with long term ground temperature modelling of ground source heat pumps. Applied Energy, (2016)

Magraner, T. 'Validación experimental de los métodos de diseño de instalaciones de bomba de calor acoplada al terreno'. Tesis Doctoral (2010)

Miglani, S., Orehounig, K., Carmeliet, J.: A methodology to calculate long-term shallow geothermal energy potential for an urban neighborhood. Energy and Buildings, (2018)

RETScreen International. Ground-source heat pump project analysis. Ministry of Natural Resources Canada

The Council European Parliament. An EU strategy on heating and cooling [Internet]. 2016. Available from: https://ec.europa.eu/transparency/regdoc/rep/1/2016/EN/1-2016-51-EN-F1-1.PDF

Acknowledgements

The authors would like to express our acknowledgment to Dr. Teresa Magraner, and to the Energesis Centro S.A. company for providing the experimental data for this study.